PRediction Of Geospace Radiation Environment and Solar wind parameterS

Work Package 6
Forecast of the radiation belt environment

Deliverable 6.1
NARMAX modelling of energetic electron fluxes at GEO

Richard Boynton, Michael Balikhin, Simon Walker, Natalia Ganushkina

June 26, 2015

This project has received funding from the *European Union's Horizon 2020 research and innovation programme* under grant agreement No 637302.

Document Change Record

Issue	Date	Author	Details
1.0	26/06/2015	R. J. Boynton	Initial draft

1 Introduction

Work Package 6 is devoted to pioneering the development of a novel forecasting technique. This is based on the fusion of system identification models of the electron fluxes with a physics based numerical model. The physics based models have an advantage of being able to model the whole region of the radiation belts. Since we do not have a complete understanding of the physics of the radiation belts, models based on first principals struggle to capture the variable dynamics of the system. While the system identification based radiation belt models provide an accurate forecast of the electron fluxes at GEO but, due to the lack of continuous data outside GEO, cannot be extended to the whole radiation belts.

The main goal of this deliverable is to develop models that extend the energy ranges of the current Sheffield model, SNB^{3}GEO and also increase the temporal resolution of the forecasts. These models will then be utilised with physics based VERB models to develop a hybrid model that will cover the whole radiation belts and have a high forecast accuracy. Therefore, the hybrid model will have the advantages of both system identification models and physics based models.

2 Conclusion

The aim of this study was to create forecast models for the electron flux energy ranges observed by the third generation GOES satellites. Also these models should have an increased temporal resolution over the $>$ 800 keV and $>$ 2 MeV GEO electron fluxes models that were previously developed Boynton et al. [2015] and are operated at Sheffield (www.ssg.group.shef.ac.uk/USSW/UOSSW.html). As such, this study has deduced five new 1 hour resolution models for the low energy electron measured by GOES, ranging in energy from 30 keV to 600 keV and extended the existing $>$ 800 keV and $>$ 2 MeV GEO electron fluxes models to forecast at a 1-hour resolution.

References

R. J. Boynton, M. A. Balikhin, and S. A. Billings. Online narmax model for electron fluxes at geo. *Ann. Geophys.*, 33(3):405–411, March 2015. ISSN 1432-0576. URL `http://www.ann-geophys.net/33/405/2015/`.

JOURNAL OF GEOPHYSICAL RESEARCH, VOL. ???, XXXX, DOI:10.1029/,

Set of NARMAX electron flux models for different energies at GEO

R. J. Boynton,[1] M. A. Balikhin,[1] D. G. Sibeck,[2] S. N. Walker,[1] S. A. Billings,[1] N. Ganushkina,[3]

R. J. Boynton, Department of Automatic Control and Systems Engineering, University of Sheffield, Mappin Street, Sheffield S1 3JD, UK. (r.boynton@sheffield.ac.uk)

[1]Department of Automatic Control and Systems Engineering, University of Sheffield, Sheffield S1 3JD, United Kingdom.

[2]NASA Goddard Space Flight Center, Greenbelt, Maryland, USA

[3]Finnish Meteorological Institute, Helsinki, Finland

Abstract. Forecast models are derived for the energetic electrons for all energy ranges sampled by the third generation Geostationary Operational Environmental Satellites (GOES). These models are based on Multi-Input Single-Output (MISO) Nonlinear AutoRegressive Moving Average with eXogenous inputs (NARMAX) methodologies. The models use solar wind and geomagnetic indices input data to produce a forecast of the energetic electrons at Geostationary Earth Orbit (GEO). These models are shown to provide accurate forecasts that are capable of warning satellite operators of when the electrons at GEO could cause problems for their spacecraft.

1. Introduction

The radiation belts consist of energetic particles trapped by the terrestrial magnetic field and were discovered by *Van Allen* [1959] from the first in situ space radiation measurements. The outer radiation belt is made up of trapped electrons ranging in energy from 10's of keV to several MeV. *Blake et al.* [1992] and *Reeves* [1998] showed that the number of these electrons can vary by several orders of magnitude in a few hours. The high fluence of these energetic electrons can cause a number of problems on spacecraft depending on the electron energy. For example, low energy electrons (10 keV to a few hundred keV) can cause surface charging that interferes with the satellite electronic systems, while higher energies (about 1 MeV and above) cause deep dielectric charging that may permanently damage the dielectric material onboard the satellite.

There are still many unanswered questions about the mechanisms involved within the radiation belts, such as the acceleration mechanisms and loss processes of the electrons. Since we do not have a complete understanding of the physics, radiation belt models based on first principals struggle to capture the variable dynamics of the system. As such, these models often have large errors between the forecast and the observed electron population.

The system identification approach has also been applied to modelling the radiation belts. In this approach, models are automatically deduced from input-output data by the system identification algorithms. These algorithms include linear prediction filters *Baker et al.* [1990], neural networks [*Koons and Gorney*, 1991; *Freeman et al.*, 1998; *Ling et al.*, 2010], and Nonlinear AutoRegressive Moving Average with eXogenous inputs (NARMAX) [*Wei et al.*, 2011; *Boynton et al.*, 2013a, 2015]. NARMAX and neural networks can both provide accurate and reliable models for nonlinear systems such as the radiation belts, however, NARMAX has the advantage of interpretability over neural networks. Neural networks result in the relationship between input and output measurements being described through a maze of multilayered neurones, in which each connection has an associated weight factor and each neurone has an activation function. This makes neural networks extremely difficult to interpret, i.e., to find out how the input variables couple together to produce changes in the output. In contrast, NARMAX models can result in a simple polynomial, from which an understanding how the inputs change the output is intuitive. Therefore, this study uses the NARMAX methodologies to model the electron fluxes observed by the Geostationary Operational Environmental Satellites (GOES).

The main aim of this study is to create reliable forecast models for the electron flux energy ranges observed by the third generation GOES satellites. The second aim is to increase temporal resolution of the forecast to that which currently operates on the University of Sheffield Space Weather Website and was developed by *Boynton et al.* [2015]. In Section 2, we discuss the methodology used to deduce the forecast models. This includes a brief description of the NARMAX algorithm. Section 3 deals with the extension of the current 24-hour resolution > 800 keV and > 2 MeV GEO electron flux models, developed by *Boynton et al.* [2015], to 1-hour resolution and their performance is calculated. In Section 4, the methodology and data used to derive the low energy models is detailed and the results of the models performances are shown. The limitations of the models and their performance are discussed in Section 5 and the study is concluded in Section 6.

2. NARMAX Methodology

As stated in Section 1, NARMAX models provide reliable forecasts and are also easy to interpret. As such, the methodology has been applied to a wide range of scientific fields, from analysing the adaptive changes in the photoreceptors of Drosophila Flies [*Friederich et al.*, 2009] to modelling the tide at the Venice Lagoon [*Wei and Billings*, 2006]. In the field of space physics, the methodology was first used to model the Dst Index using the half wave rectifier as the input [*Balikhin et al.*, 2001; *Boaghe et al.*, 2001]. More recently, due to absence of knowledge about the inputs to the Dst index system, *Boynton et al.* [2011b] used the NARMAX model structure detection methodology to identify the main control parameter, or solar wind coupling function, for geomagnetic storms quantified using the Dst index. *Boynton et al.* [2011a] used this coupling function to deduce a reliable model for the Dst Index. *Boynton et al.* [2013b] and *Balikhin et al.* [2011] employed a similar approach to identify the solar wind control parameters for electron fluxes at GEO. The interpretability of these results allowed *Balikhin et al.* [2012] to make a direct comparrison with the energy diffusion equation, where they found that acceleration due to local diffusion is not dominant at GEO.

NARMAX models were first proposed by *Leontaritis and Billings* [1985a, b] who demonstrated the models have the potential to represent a wide class of nonlinear systems. A Multi-Input Single-Output (MISO) NARMAX model, which was used in this study to model the electron fluxes at GEO, is expressed by

$$\begin{aligned} y(t) \; = \; & F[y(t-1), ..., y(t-n_y), \\ & u_1(t-1), ..., u_1(t-n_{u_1}), ..., \\ & u_m(t-1), ..., u_m(t-n_{u_m}), ..., \\ & e(t-1), ..., e(t-n_e)] + e(t) \end{aligned} \tag{1}$$

where y, u, and e represent the output, input and error terms respectively, $F[\cdot]$ represents some nonlinear function (a polynomial in the case of this study), m is the number of system inputs and n_y, n_{u_1},..., n_{u_m}, n_e are the maximum time lags for the output, each of the m inputs, and the error respectively.

Billings et al. [1988] developed the first Forward Regression Orthogonal Least Squares (FROLS) algorithm that automatically fits a NARMAX model using input-output training data sets. Simply put, the overall algorithm put forward by *Billings et al.* [1988] involved three stages. The first stage is model structure detection, which identifies the variables or combination of variables that control the evolution of the system. In Equation 1, the expansion of $F[\cdot]$ in terms of a high degree polynomial, results in a huge number of monomials, especially if there are many possible inputs. The vast majority of the possible monomials will have little influence on the system, i.e., the coefficients of the monomial will be zero. Therefore, only a small number of monomials are required to represent the dynamics of the system. The FROLS procedure identifies the most significant monomials by use of the Error Reduction Ratio (ERR). Once the model structure is detected, the second stage is to estimate the coefficient for each of the monomials detected in the model. These first two stages are referred to as training the model. The final stage is to validate the model. Since its inception, there have many variants on the FROLS algorithm [*Billings et al.*, 1989; *Mao and Billings*, 1997; *Wei and Billings*, 2008]. This study employes the Iterative Orthogonal Forward Regression (IOFR) algorithm, developed by *Guo et al.* [2014], which is more likely to detect the optimal model when the data is oversampled.

3. Increasing the time resolution of the existing > 800 keV and > 2 MeV GEO electron flux models

Models for forecasting the fluxes of > 800 keV and > 2 MeV electrons at GEO were developed by *Boynton et al.* [2015]. These models were deduced using the NARMAX methodology and provide a 1-day resolution forecast for one day ahead. Both of these models were shown to have a high prediction efficiency for estimating the next days electron flux value [*Boynton et al.*, 2015]. The forecast results can be found online at www.ssg.group.shef.ac.uk/USSW/UOSSW.html.

One of the aims of this study is to increase the temporal resolution of these forecasts. Therefore, the temporal resolution of the > 800 keV and > 2 MeV GEO electron flux models were extended to give a forecast of the electron fluxes every hour for the next 24 hours in contrast only one daily forecast per day.

3.1. Data and methodology

The > 800 keV and > 2 MeV electron flux models rely on solar wind inputs to forecast the electron flux. The solar wind inputs are the daily average velocity and density; and the amount of time the IMF is southward in a 24 hour period. The 1-minute solar wind velocity, density and IMF z-component data were obtained from the OMNI website (http://omniweb.gsfc.nasa.gov/ow_min.html) from 1 January 2011 to 28 February 2015. At every hour, the past 24 hour average of the solar wind velocity and density was calculated. For example, the point at 10:00:00 UTC on 5 January 2015 is average of the 1440 1-minute points between 10:01:00 UTC on 4 January 2015 and 10:00:00 UTC on 5 January 2015. In addition, the number of minutes that the IMF was southward during the past 24 hours was determined for the final input.

The electron flux data used to analyse the performance of the extended temporal resolution $>$ 800 keV and $>$ 2 MeV GEO electron flux models were from the third generation GOES satellite, GOES 13. The electron fluxes onboard the GOES 13 satellite are measured by the Energetic Proton Electron and Alpha Detector (EPEAD) [*Hanser*, 2011] and the MAGnetospheric Electron Detector (MAGED) [*Hanser*, 2011]. The data for these instruments can be accessed from http://www.ngdc.noaa.gov/stp/satellite/goes/dataaccess.html.

The EPEAD measures the relativistic integral electron fluxes and has two detectors pointing in opposite directions, tangential to the spacecrafts orbit and are named the East and West detectors. These data were used to assess the 1-hour temporal resolution of the SNB^{3}GEO electron flux models. The data period used for this part of the study was from 1 January 2011 to 28 February 2015. The study employed the $>$ 800 keV and $>$ 2 MeV energy channels from both the east and west detector onboard the GOES 13 satellite. The 5-minute proton corrected electron flux values were averaged between the east and west detector to get an omnidirectional flux. This was then temporally averaged resulting in a data set with 1-hour resolution, such that each 1-hour point was determined by averaging the 5-minute omnidirectional data over the past 24 hours, e.g the point at 10:00:00 UTC on 5 January 2015 is average of the 288 5-minute points between 10:05:00 UTC on 4 January 2015 and 10:00:00 UTC on 5 January 2015. This data would then be compared to the model forecast.

3.2. Model Performance

The $>$ 800 keV and $>$ 2 MeV GEO electron flux models were run using the 1-hour resolution input data and the results were compared to the EPEAD 1-hour electron flux data, for the period from from 1 January 2011 to 28 February 2015. The performance of the models during the period could then be analysed.

The performance of the models was assessed statistically by the the Correlation Coefficient (CC), Eq. (2), and the Prediction Efficiency (PE), Eq. (3), which are commonly used to assess models [*Temerin and Li*, 2006; *Li*, 2004; *Boynton et al.*, 2011a; *Wei et al.*, 2004; *Boynton et al.*, 2015; *Rastatter et al.*, 2013].

$$\rho_{y\hat{y}} = \frac{\sum_{t=1}^{N}\left[\left(y(t)-\bar{y}\right)\left(\hat{y}(t)-\bar{\hat{y}}\right)\right]}{\sqrt{\sum_{t=1}^{N}\left[\left(y(t)-\bar{y}\right)^2\right]\sum_{t=1}^{N}\left[\left(\hat{y}(t)-\bar{\hat{y}}\right)^2\right]}}100\% \tag{2}$$

$$E_{PE} = \left[1-\frac{\sum_{t=1}^{N}\left[\left(y(t)-\hat{y}(t)\right)^2\right]}{\sum_{t=1}^{N}\left[\left(y(t)-\bar{y}\right)^2\right]}\right]100\% \tag{3}$$

Here, E_{PE} is the PE, ρ is the CC, $y(t)$ is the output at time t, $\hat{y}$ is the estimated output from the model, N is the length of the data and the bar signifies the average.

3.2.1. > 800 keV model

Figure 1 shows the past 24 hour average > 800 keV electron flux measured by GOES in blue and the model 24 hour ahead forecast in orange for the period from 1 January 2011 to 28 February 2015. During this period, the model the PE was 72.1% and the CC was 85.1%.

3.2.2. > 2 MeV model

Figure 2 shows the past 24 hour average > 2 MeV electron flux measured by GOES in blue and the model 24 hour ahead forecast in orange for the period from 1 January 2011 to 28 February 2015. The PE for the > 2 MeV model was 82.3% while the CC was 90.9%.

Figure 2 reflects the statistics, since it can clearly be seen that the model closely follows the blue observed GOES electron flux, which is seen more when the electron flux is low.

4. Modelling the low energy electron fluxes measured by third generation GOES

Models to forecast the low energy electrons measured by GOES satellites were deduced using the NARMAX IOFR algorithm. This method requires input-output data for training the models.

4.1. Data and Methodology

The electron flux data for the training and validation of these models comes again from the GOES 13 satellite. The MAGED has 9 telescopes pointing in different directions and measures the lower energy differential electron fluxes in 5 energy channels: 30-50 keV, 50-100 keV, 100-200 keV, 200-350 keV and 350-600 keV. The data period used for this part of the study was from 1 May 2010 to 28 February 2015 and employed all energy channels available from the instrument. Since this study is concerned mainly with the trapped electrons, the study used the telescope with the closest pitch angle to 90 degrees, This turned out to be telescope 3, although telescopes 1-5 all had pitch angles close to 90 degrees and over the concerned time scales, had a negligible difference in the fluxes.

Solar wind and geomagnetic indices were used as input data for training the models. The 1-minute solar wind velocity, density and IMF z-component data were obtained from the OMNI website (http://omniweb.gsfc.nasa.gov/ow_min.html), while the Dst geomagnetic index was from the World Data Center for Geomagnetism, Kyoto (http://wdc.kugi.kyoto-u.ac.jp/index.html).

4.2. Model Training

A data period was selected for the model training. The training data was from 1 March 2011 to 28 February 2013. For the training data, the 1-minute corrected electron flux values were daily averaged between 00:01:00 UTC and 00:00:00 UTC the next day for each day, resulting in training 790 data points.

The inputs to these models are more complicated in terms of prediction when compared to the $>$ 800 keV and $>$ 2 MeV energy channels. The studies by *Boynton et al.* [2013b] and *Balikhin et al.* [2012] showed that the time delay in the reaction of electron fluxes to changes in the solar wind increased with the energy. The high energy models of $>$ 800 keV and $>$ 2 MeV had minimum time delays of one day and thus it is possible to forecast one day into the future. However, the value of the solar wind in the current day will effect the low energy electron flux on the same day. Therefore, it is not possible to forecast one day ahead. To get around this problem, the past 24 hour averages were calculated for each hour, as previously described. Therefore, the input time lags in the algorithm, n_{u_m}, were shifted hourly not daily. For example, if input $U(t-10$ hours) is selected by the model, this monomial represents the average of the points between $U(t-10$ hours) and $U(t-34$ hours).

The algorithm was run for the 5 energy ranges using lagged inputs from 2 to 48 hours. These inputs were the solar wind velocity and density, the amount of time the IMF is southward in a 24 hour period, the Dst index, and the term resulting from the coupling function proposed by *Balikhin et al.* [2010] and *Boynton et al.* [2011b], $B_T \sin^6(\theta/2)$ (where $B_T = \sqrt{(}B_y^2 + B_z^2)$ is the tangential IMF and $\theta = \tan^{-1}(B_y/B_z)$ is the clock angle of the IMF).

For the 30-50 keV, a compromise had to be made between producing a reliable forecast and the amount of time the model can forecast into the future. The model detected by the algorithm included input terms with a 6 hour time lag and thus could only forecast 6 hours into the future. To increase the length of the forecast, the ≤ 6 hour time lagged monomials were manually removed from the algorithms search to see if the performance of the model, based on PE and the CC, dropped significantly. It was found there was only a negligible drop in performance if the detected model had input terms with a minimum of 7 hour time lag. This process of removing monomials with larger and larger time lags was continued until there was a significant performance drop in the model output. This occurred after $t-9$ hour time lags were removed from the search, resulting in inputs with a minimum time lag of 10 hours. This was used as the final 30-50 keV model and could forecast the past 24 hour average of the flux 10 hours in the future. This methodology was repeated for the other 4 energy channels and as with the studies by *Boynton et al.* [2013b] and *Balikhin et al.* [2012], the time delay of electron fluxes increased with the energy.

4.3. Final Model Performance

The performance of the models were analysed statistically using the PE and CC. Each of the models were run on the data from 1 March 2013 to 28 February 2015. At first the models were run on the daily averaged data which results in 730 points for the period. Then the models were extended to 1-hour resolution of the past 24 hour average, which contains 17520 points, to assess the models performance with an increase of the temporal resolution.

Table 1 lists the performance of the five low energy electron flux models, showing the PE and CC on the 1-day resolution data and the PE and CC on the 1-hour resolution data. The Table also shows the minimum time lag used in the model and thus how far ahead the model can forecast into the future. This is in agreement with the studies by *Boynton et al.* [2013b] and *Balikhin et al.* [2012], since the minimum time lags increase with energy. The results of the five models on the 1-hour resolution data are illustrated in Figures 3 (30-50 keV model), 4 (50-75 keV model), 5 (100-200 keV model), 6 (200-350 keV model) and 7 (350-600 keV model). The Figures show the observed GOES electron flux in blue and the model forecast in orange.

5. Discussion

One of the aims of this study was to increase the temporal resolution of the forecasts of the $>$ 800 keV and $>$ 2 MeV GEO electron fluxes models that currently operate online. These models provide daily averaged one day ahead forecasts for each UTC day. Increasing the resolution of the model by using one hour averages of the GOES data is not that simple because during a 24 hour GEO orbit there is a significant spatial variation of the electron fluxes that is independent of any temporal changes due to adiabatic acceleration and loss. This is due to changes in the structure of the terrestrial magnetic field, where compressions on the dayside increase the strength of magnetic field and thus accelerate the electrons. Therefore, higher fluxes are observed when GOES is situated at noon compared to midnight were the magnetic field is weaker at GEO. This spatial variation makes it difficult to deduce a data based model because the satellites position is always changing. As such, to achieve the aim of increasing the temporal resolution, we employed a moving average of the preceding 24 hours calculated every hour. We applied the existing $>$ 800 keV and > 2 MeV GEO electron fluxes models to this 1-hour averaged data because these models have already been proven to be reliable in their online operation (Balikhin et al., [2015] submitted to Space Weather). This change in input time resolution resulted in high values for the PE and CC, higher than those reported by *Boynton et al.* [2015]. *Boynton et al.* [2015] showed, using the 1-day resolution data, that the > 2 MeV model had a PE of 78.6% and a CC of 89.4% and that the > 800 keV model had a PE of 70% and a CC of 84.7% between the 1 January 2011 and 30 June 2012, all of which are lower than the results shown in this study. However, these statistics should really be compared over the same time time period. Based on the time period between the 1 January 2011 and 30 June 2012 the 1 hour PE was 76.0% and the CC was 87.5% for the > 800 keV model and the PE was 82.3% and the CC was 90.8% for the > 2 MeV model. Therefore, these models perform better using the 1-hour resolution data. This was also the case for three out of the five lower energy models. Only the two lowest energy models performed worse on the 1-hour resolution data.

One of the limitations of the three lowest energy models is that they forecast less time into the future than the higher energy models, since the low energy electron fluxes at GEO respond to solar wind changes significantly faster than high energy electrons [*Balikhin et al.*, 2012; *Boynton et al.*, 2013b]. The 30-50 keV model is only able to forecast the 24 hour average electron flux 10 hours into the future, which means that 14 hours of this average is already measured. Also, it should be noted that better models with higher performance statistics for the MAGED models, except for the 350-600 keV energy channel, could be obtained if the forecast length was sacrificed. For example, the 30-50 keV model had a 4% higher PE if 6 hour time lags were included in the algorithm but this would mean that 18 hours of the forecast had already been measured by GOES.

6. Conclusions

The aim of this study was to create forecast models for the electron flux energy ranges observed by the third generation GOES satellites, which have an increased temporal resolution over the $>$ 800 keV and $>$ 2 MeV GEO electron fluxes models that were previously developed *Boynton et al.* [2015]. As such, this study has deduced five new 1-hour resolution models for the low energy electrons measured by GOES, ranging in energy from 30 keV to 600 keV and extended the existing $>$ 800 keV and $>$ 2 MeV GEO electron fluxes models to forecast at a 1-hour resolution.

All of these models will be implemented in real time to forecast the electron fluxes on the University of Sheffield Space Weather website (www.ssg.group.shef.ac.uk/USSW/UOSSW.html).

Acknowledgments. Solar wind data was obtained from OMNIweb (http://omniweb.gsfc.nasa.gov/ow_r Dst index data from the World Data Center for Geomagnetism, Kyoto (http://wdc.kugi.kyoto-u.ac.jp/index.html) and GOES data from the Nation Oceanic and Atmospheric Administration (http://www.ngdc.noaa.gov/stp/satellite/goes/dataaccess.html). This project has received funding from the European Union's Horizon 2020 research and innovation programme under grant agreement No 637302.

References

Baker, D. N., R. L. McPherron, T. E. Cayton, and R. W. Klebesadel, Linear prediction filter analysis of relativistic electron properties at 6.6 re, *J. Geophys. Res.*, *95*(A9), 15,133–15,140, 1990.

Balikhin, M. A., O. M. Boaghe, S. A. Billings, and H. S. C. K. Alleyne, Terrestrial magnetosphere as a nonlinear resonator, *Geophys. Res. Lett.*, *28(6)*, 11231126, 2001.

Balikhin, M. A., R. J. Boynton, S. A. Billings, M. Gedalin, N. Ganushkina, D. Coca, and H. Wei, Data based quest for solar wind-magnetosphere coupling function, *Geophys. Res. Lett.*, *37*(24), L24,107, 2010.

Balikhin, M. A., R. J. Boynton, S. N. Walker, J. E. Borovsky, S. A. Billings, and H. L. Wei, Using the narmax approach to model the evolution of energetic electrons fluxes at geostationary orbit, *Geophys. Res. Lett.*, *38*(18), L18,105, 2011.

Balikhin, M. A., M. Gedalin, G. D. Reeves, R. J. Boynton, and S. A. Billings, Time scaling of the electron flux increase at geo: The local energy diffusion model vs observations, *J. Geophys. Res.*, *117*(A10), A10,208–, 2012.

Billings, S., M. Korenberg, and S. Chen, Identification of non-linear output affine systems using an orthogonal least-squares algorithm., *Int. J. of Systems Sci.*, *19*, 1559–1568, 1988.

Billings, S., S. Chen, and M. Korenberg, Identification of mimo non-linear systems using a forward-regression orthogonal estimator, *Int. J. Control*, *49(6)*, 2157–2189, 1989.

Blake, J. B., W. A. Kolasinski, R. W. Fillius, and E. G. Mullen, Injection of electrons and protons with energies of tens of mev into l¡3 on 24 march 1991, *Geophys. Res. Lett.*, *19*(8), 821–824, 1992.

Boaghe, O. M., M. A. Balikhin, S. A. Billings, and H. Alleyne, Identification of nonlinear processes in the magnetospheric dynamics and forecasting of dst index, *J. Geophys. Res.*, *106(A12)*, 30,04730,066, 2001.

Boynton, R. J., M. A. Balikhin, S. A. Billings, A. S. Sharma, and O. A. Amariutei, Data derived narmax dst model, *Annales Geophysicae*, *29*(6), 965–971, doi:10.5194/angeo-29-965-2011, 2011a.

Boynton, R. J., M. A. Balikhin, S. A. Billings, H. L. Wei, and N. Ganushkina, Using the narmax ols-err algorithm to obtain the most influential coupling functions that affect the evolution of the magnetosphere, *J. Geophys. Res.*, *116*(A5), A05,218, 2011b.

Boynton, R. J., M. A. Balikhin, S. A. Billings, and O. A. Amariutei, Application of nonlinear autoregressive moving average exogenous input models to geospace: advances in understanding and space weather forecasts, *Ann. Geophys.*, *31*(9), 1579–1589, 2013a.

Boynton, R. J., M. A. Balikhin, S. A. Billings, G. D. Reeves, N. Ganushkina, M. Gedalin, O. A. Amariutei, J. E. Borovsky, and S. N. Walker, The analysis of electron fluxes at geosynchronous orbit employing a narmax approach, *J. Geophys. Res. Space Physics*, *118*(4), 1500–1513, 2013b.

Boynton, R. J., M. A. Balikhin, and S. A. Billings, Online narmax model for electron fluxes at geo, *Ann. Geophys.*, *33*(3), 405–411, 2015.

Freeman, J. W., T. P. O'Brien, A. A. Chan, and R. A. Wolf, Energetic electrons at geostationary orbit during the november 3-4, 1993 storm: Spatial/temporal morphology, characterization by a power law spectrum and, representation by an artificial neural network, *J. Geophys. Res.*, *103*(A11), 26,251–26,260, 1998.

Friederich, U., D. Coca, S. A. Billings, and M. Juusola, Data modelling for analysis of adaptive changes in fly photoreceptors, *NEURAL INFORMATION PROCESSING, PT 1, PROCEEDINGS*, *5863*, 34–38, 2009.

Guo, Y., L. Guo, S. Billings, and H.-L. Wei, An iterative orthogonal forward regression algorithm, *International Journal of Systems Science*, *46*(5), 776–789, doi:10.1080/00207721.2014.981237, 2014.

Hanser, F. A., Eps/hepad calibration and data handbook, *Tech. rep.*, Tech. Rep. GOESN-ENG-048D, Assurance Technol. Corp., Carlisle, Mass., 2011.

Koons, H. C., and D. J. Gorney, A neural network model of the relativistic electron flux at geosynchronous orbit, *J. Geophys. Res.*, *96*(A4), 5549–5556, 1991.

Leontaritis, I. J., and S. A. Billings, Input-output parametric models for non-linear systems part i: Deterministic non-linear systems., *Int. J. Control*, *41 (2)*, 303–328, 1985a.

Leontaritis, I. J., and S. A. Billings, Input-output parametric models for non-linear systems part ii: Stochastic nonlinear systems, *Int. J. Control*, *41 (2)*, 329–344, 1985b.

Li, X., Variations of 0.7-6.0 mev electrons at geosynchronous orbit as a function of solar wind, *Space Weather*, *2*(3), S03,006, 2004.

Ling, A. G., G. P. Ginet, R. V. Hilmer, and K. L. Perry, A neural network-based geosynchronous relativistic electron flux forecasting model, *Space Weather*, *8*(9), S09,003–, 2010.

Mao, K. Z., and S. A. Billings, Algorithms for minimal model structure detection in nonlinear dynamic system identification, *International Journal of Control*, *68*(2), 311–330, doi:10.1080/002071797223631, 1997.

Rastatter, L., M. M. Kuznetsova, A. Glocer, D. Welling, X. Meng, J. Raeder, M. Wiltberger, V. K. Jordanova, Y. Yu, S. Zaharia, R. S. Weigel, S. Sazykin, R. Boynton, H. Wei, V. Eccles, W. Horton, M. L. Mays, and J. Gannon, Geospace environment modeling 2008-2009 challenge: Dst index, *Space Weather*, *11*(4), 187–205, 2013.

Table 1. Table showing the performance of the five low energy electron flux models as well as the

Model	Forecast Time	1-day PE (%)	1-day CC (%)	1-hour PE (%)	1-hour CC (%)
30-50 keV	10 hr	72.0	84.9	66.9	82.0
50-100 keV	12 hr	70.6	84.2	69.2	83.5
100-200 keV	16 hr	71.1	84.4	72.2	85.6
200-350 keV	24 hr	69.5	83.7	71.6	84.9
350-600 keV	24 hr	69.9	83.8	73.7	85.9

Reeves, G. D., Relativistic electrons and magnetic storms: 1992-1995, *Geophys. Res. Lett.*, *25*(11), 1817–1820, 1998.

Temerin, M., and X. Li, Dst model for 1995 - 2002, *J. Geophys. Res.*, *111*(A4), A04,221, 2006.

Van Allen, J. A., The geomagnetically trapped corpuscular radiation, *J. Geophys. Res.*, *64*(11), 1683–1689, 1959.

Wei, H. L., and S. A. Billings, An efficient nonlinear cardinal b-spline model for high tide forecasts at the venice lagoon, *Nonlinear Processes In Geophysics*, *13*(5), 577–584, 2006.

Wei, H.-L., and S. A. Billings, Model structure selection using an integrated forward orthogonal search algorithm assisted by squared correlation and mutual information, *Int. J. Modelling, Identification and Control*, *3*, 341–356, 2008.

Wei, H. L., S. A. Billings, and M. Balikhin, Prediction of the dst index using multiresolution wavelet models, *J. Geophys. Res.*, *109*(A7), A07,212, 2004.

Wei, H.-L., S. A. Billings, A. Surjalal Sharma, S. Wing, R. J. Boynton, and S. N. Walker, Forecasting relativistic electron flux using dynamic multiple regression models, *Annales Geophysicae*, *29*(2), 415–420, doi:10.5194/angeo-29-415-2011, 2011.

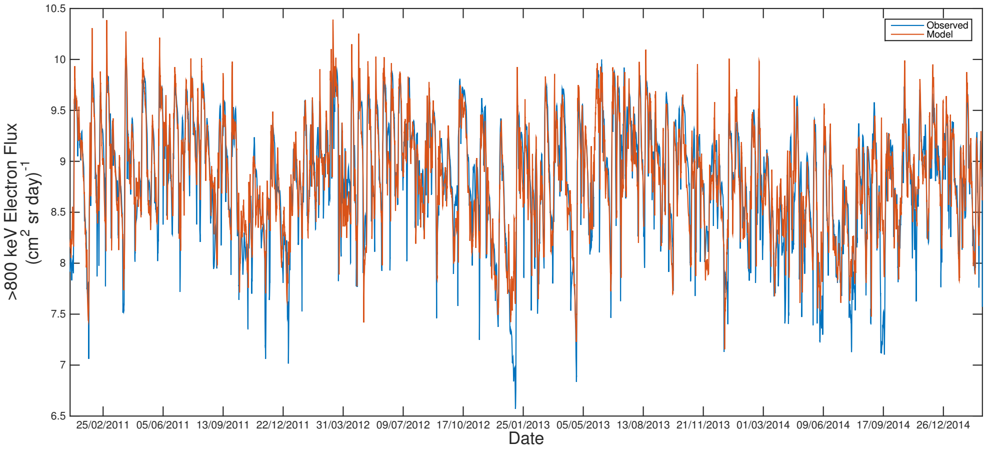

Figure 1. The past 24 hour average > 800 keV electron flux measured by GOES in blue and the model 24 hour ahead forecast in orange for the period from 1 January 2011 to 28 February 2015

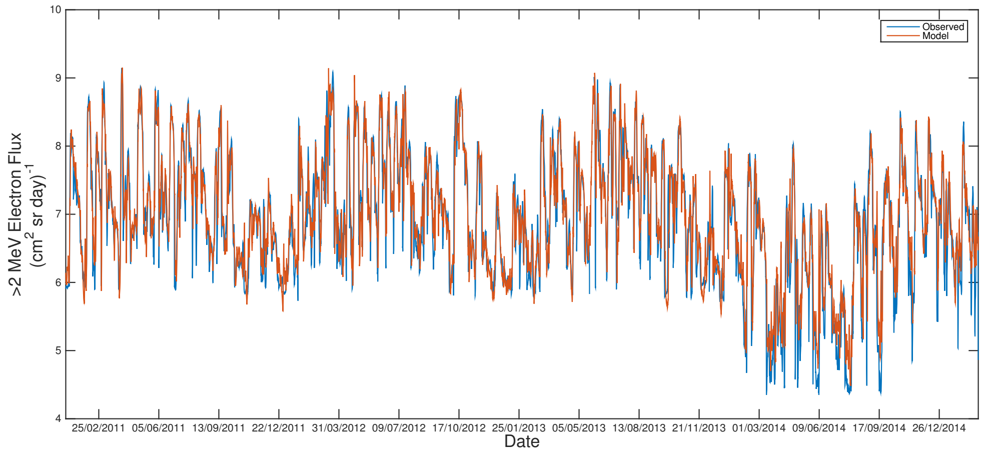

Figure 2. The past 24 hour average > 2 MeV electron flux measured by GOES in blue and the model 24 hour ahead forecast in orange for the period from 1 January 2011 to 28 February 2015

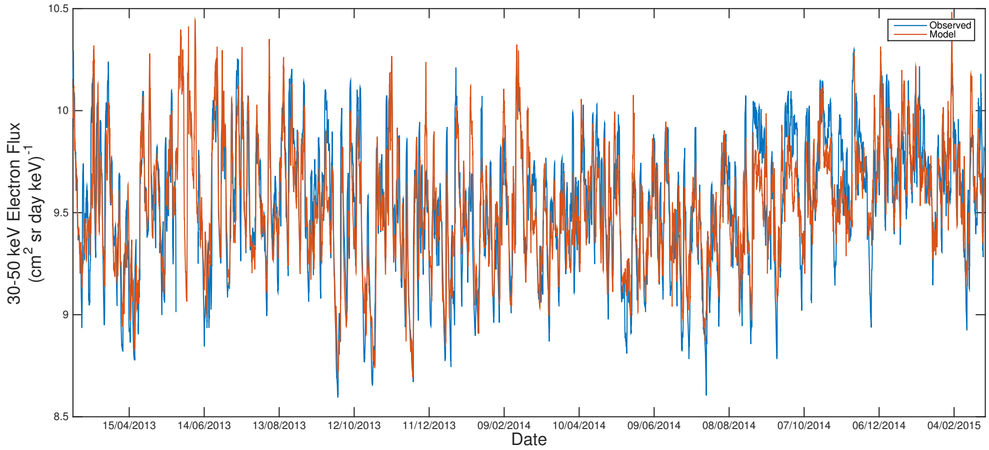

Figure 3. The daily average 30-50 MeV electron flux measured by GOES in blue and the model 24 hour ahead forecast in orange for the period from 1 March 2013 to 28 February 2015

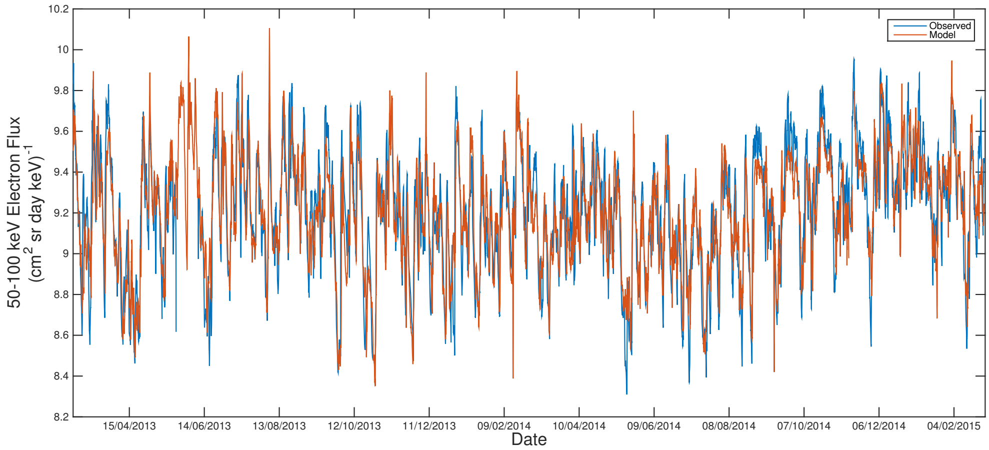

Figure 4. The daily average 50-100 MeV electron flux measured by GOES in blue and the model 24 hour ahead forecast in orange for the period from 1 March 2013 to 28 February 2015

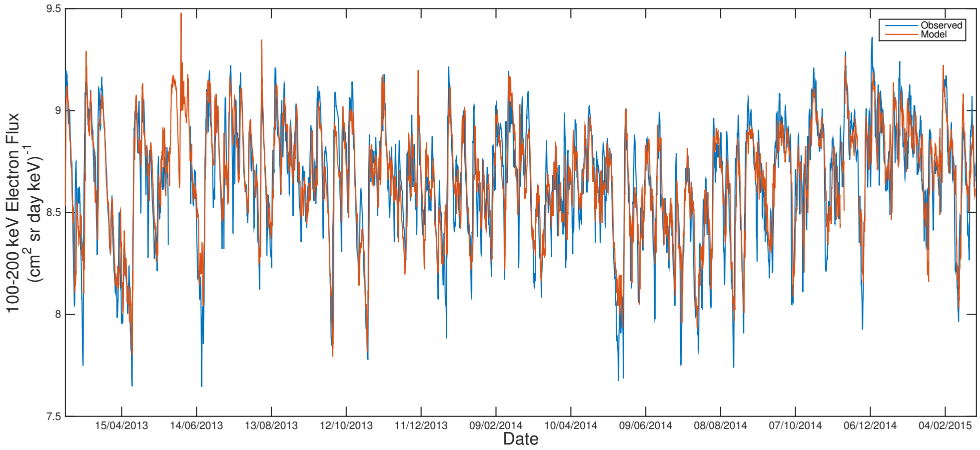

Figure 5. The daily average 100-200 MeV electron flux measured by GOES in blue and the model 24 hour ahead forecast in orange for the period from 1 March 2013 to 28 February 2015

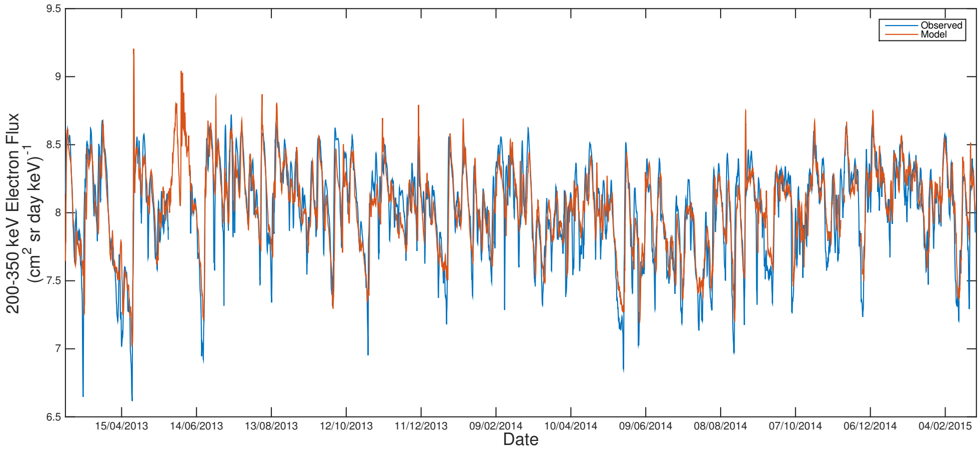

Figure 6. The daily average 200-350 MeV electron flux measured by GOES in blue and the model 24 hour ahead forecast in orange for the period from 1 March 2013 to 28 February 2015

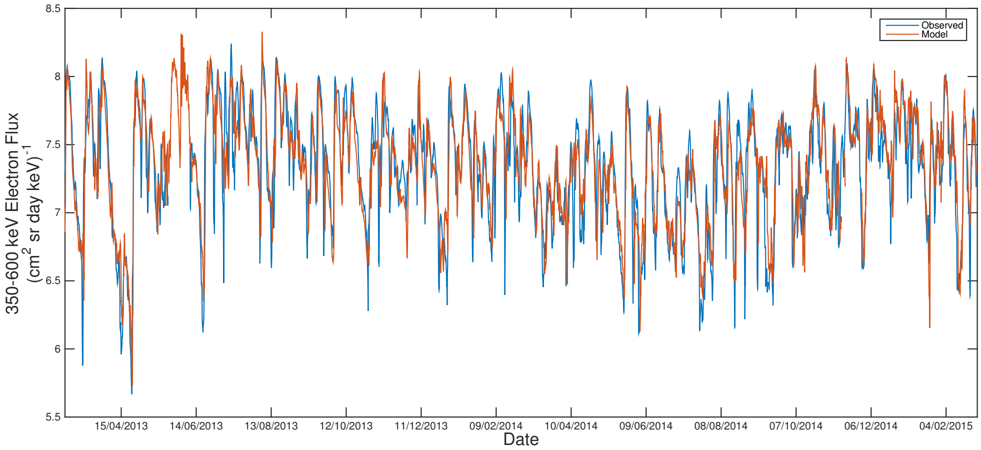

Figure 7. The daily average 350-600 MeV electron flux measured by GOES in blue and the model 24 hour ahead forecast in orange for the period from 1 March 2013 to 28 February 2015